

Electroweak dark matter model accounting for the CDF W -mass anomaly

Jin-Wei Wang^{1,2,3,*}, Xiao-Jun Bi^{4,5,†}, Peng-Fei Yin^{4,‡} and Zhao-Huan Yu^{6,§}

¹*Scuola Internazionale Superiore di Studi Avanzati (SISSA), via Bonomea 265, 34136 Trieste, Italy*

²*INFN, Sezione di Trieste, via Valerio 2, 34127 Trieste, Italy*

³*Institute for Fundamental Physics of the Universe (IFPU), via Beirut 2, 34151 Trieste, Italy*

⁴*Key Laboratory of Particle Astrophysics, Institute of High Energy Physics,
Chinese Academy of Sciences, Beijing 100049, China*

⁵*School of Physical Sciences, University of Chinese Academy of Sciences, Beijing 100049, China and*

⁶*School of Physics, Sun Yat-Sen University, Guangzhou 510275, China*

Recently, the CDF collaboration reported a new measurement of the W boson mass $M_W = 80.4335 \pm 0.0094$ GeV, which shows a $\sim 7\sigma$ deviation from the standard model prediction 80.3545 ± 0.0057 GeV obtained by the electroweak (EW) global fit. This deviation can be explained by new physics generating moderate EW oblique parameters S , T , and U . In this work, we use the loop corrections induced by some extra EW multiplets to explain the CDF M_W anomaly. The lightest neutral particle in the multiplets can also serve as a candidate of cold dark matter (DM). We consider two such models, namely singlet-triplet scalar DM and singlet-doublet fermionic DM models, and perform numerical scans to find the parameter points accounting for the M_W anomaly. The constraints from the correct DM thermal relic density and direct detection are also taken into account. We find the parameter points simultaneously interpreting the M_W anomaly and satisfying the DM requirements in the former model, but do not find such parameter points in the latter model.

* jinwei.wang@sissa.it

† bixj@ihep.ac.cn

‡ yinpf@ihep.ac.cn

§ yuzhaoh5@mail.sysu.edu.cn

I. INTRODUCTION

Electroweak (EW) precision observables are important and powerful probes for exploring the new physics (NP) beyond the standard model (SM). Choosing some observables as input parameters, such as the fine structure constant α , the Z boson mass M_Z , and the Fermi coupling constant G_F , other observables including the W boson mass M_W can be precisely predicted in the SM with radiative corrections. Any deviation of these measured observables from the SM prediction may provide a hint of NP.

Recently, the CDF collaboration reported an updated result of the direct measurement of the W boson mass [1],

$$M_W = 80.4335 \pm 0.0064_{\text{stat}} \pm 0.0069_{\text{syst}} \text{ GeV} = 80.4335 \pm 0.0094 \text{ GeV}, \quad (1)$$

using 8.8 fb^{-1} of data at the proton-antiproton collider Tevatron. Compared with the previous measurements performed by D0 [2], ATLAS [3], LHCb [4], and CDF itself [5], and the world average $M_W^{\text{ave}} = 80.379 \pm 0.0012 \text{ GeV}$ [6], the new CDF M_W result has a smaller uncertainty but a much higher central value. This result also shows a significant deviation $\sim 7\sigma$ from the SM prediction $M_W^{\text{SM}} = 80.3545 \pm 0.0057 \text{ GeV}$ obtained by the EW global fit [7], while the results of other EW measurements are basically consistent with the SM prediction. In order to confirm the deviation of M_W , more precise measurements are required in the future.

If the deviation of M_W given by CDF is true, then it would be an evidence of NP at the EW sector, providing a very rich phenomenology [8–83]. The universal framework of the effective field theory is helpful for understanding the properties of the corresponding NP. The general NP effects on the EW observables can be described by some well-known parameters, such as EW oblique parameters S , T , and U [84, 85]. Through the global fit including the contributions of $\text{SU}(2)_L$ invariant dimension-6 operators, some groups have pointed out that the NP effects generating $|H^\dagger D_\mu H|^2$ with $T \gtrsim 0.1$ can easily explain the CDF M_W anomaly [10, 13, 15, 23, 28, 34, 43]. Such interpretation can be realized by either the tree-level NP contributions at a few TeV or the loop-level NP contributions at a few hundred GeV in many specific models.

It is obvious that the introduction of new EW multiplets could affect the EW precision observables through loop corrections (e.g., Refs. [86–90]). The lightest neutral NP particle in these multiplets could be a kind of so-called weakly interacting massive particles, serving as a candidate of cold dark matter (DM) under a Z_2 symmetry. On the other hand, the NP particles in the extra multiplets may also couple to the Higgs boson and affect its properties, such as the Higgs production and decay rates at colliders [91–93] and the vacuum stability [94–98]. Therefore, such models would provide a very rich phenomenology at both the particle physics and astrophysical detection [99–117].

In this work, we study the CDF M_W anomaly in two DM models involving new $\text{SU}(2)_L$ multiplets, namely the singlet-triplet scalar DM (STSDM) [90] and singlet-doublet fermionic DM (SDFDM) [86, 99, 101] models. In the STSDM model, an inert real scalar singlet and an inert complex scalar triplet are introduced. We perform a random scan in the 8-dimensional parameter

space, and find the parameter points accounting for the CDF M_W anomaly and satisfying the DM relic density observation and direct detection constraints.

The SDFDM model involves a Weyl singlet and two Weyl doublets. We perform a scan in the 4-dimensional parameter space of this model. However, no parameter point simultaneously explaining the CDF M_W anomaly and fulfilling the DM phenomenological requirements is found in the scan. We explore the reason for this result in detail and perform some checks to confirm this result. Generally speaking, compared with fermionic models, scalar models have more interactions between the NP particles and the Higgs boson. Therefore, scalar models have more free parameters to help satisfy all experimental requirements.

This paper is organized as follows. In Sec. II we introduce the STSDM model and the framework for calculating the corrections to M_W . Then a random scan is carried out to find the parameter points simultaneously interpreting the CDF M_W anomaly and satisfying the DM requirements. In Sec. III, we introduce the SDFDM model, and discuss why there do not exist parameter points satisfying both the requirements of the M_W anomaly and DM phenomenology. Finally, the discussions and conclusions are given in Sec. IV.

II. THE STSDM MODEL

A. Model

The STSDM model [90] contains an inert real scalar singlet S and an inert complex scalar triplet Δ . They do not carry hypercharge, living in the following $SU(2)_L \times U(1)_Y$ representations,

$$S \in (\mathbf{1}, 0), \quad \Delta = \begin{pmatrix} \Delta^+ \\ \Delta^0 \\ \Delta^- \end{pmatrix} \in (\mathbf{3}, 0). \quad (2)$$

Here S and Δ^0 are electrically neutral, while Δ^+ and Δ^- carry electric charges $Q = +1$ and $Q = -1$, respectively. The neutral component of Δ can be decomposed as $\Delta^0 = (\phi + ia)/\sqrt{2}$, where ϕ and a are real scalars. The triplet can be described by a traceless type-(1, 1) $SU(2)_L$ tensor Δ_j^i , whose components are $\Delta_{\frac{1}{2}}^{\frac{1}{2}} = \Delta^+$, $\Delta_{\frac{1}{2}}^{\frac{3}{2}} = \Delta^-$, and $\Delta_{\frac{1}{2}}^{\frac{1}{2}} = -\Delta_{\frac{3}{2}}^{\frac{1}{2}} = -\Delta^0/\sqrt{2}$. The Hermitian conjugate of Δ_j^i is denoted as $(\Delta^\dagger)_i^j \equiv (\Delta_j^i)^\dagger$, whose components are $(\Delta^\dagger)_1^2 = (\Delta^+)^\dagger$, $(\Delta^\dagger)_{\frac{1}{2}}^{\frac{1}{2}} = (\Delta^-)^\dagger$, and $(\Delta^\dagger)_1^{\frac{1}{2}} = -(\Delta^\dagger)_{\frac{1}{2}}^2 = -(\Delta^0)^\dagger/\sqrt{2}$.

In order to make sure S and Δ inert, we assume a Z_2 symmetry of $S \rightarrow -S$ and $\Delta \rightarrow -\Delta$, which remains unbroken after the breaking of EW gauge symmetry. The gauge-invariant Lagrangian for the NP sector is

$$\mathcal{L}_{\text{NP}} = \frac{1}{2}(\partial_\mu S)\partial^\mu S + [(D_\mu \Delta)^\dagger]_i^j D^\mu \Delta_j^i - V(S, \Delta), \quad (3)$$

where the scalar potential involving S and Δ is given by

$$V(S, \Delta) = \frac{1}{2}m_S^2 S^2 + m_\Delta^2 (\Delta^\dagger)_i^j \Delta_j^i + \frac{1}{2}(\mu_\Delta^2 \Delta_j^i \Delta_i^j + \text{H.c.}) + \frac{1}{2}\lambda_{Sh} S^2 H_i^\dagger H^i + \lambda_1 H_i^\dagger \Delta_j^i (\Delta^\dagger)_k^j H^k$$

$$+\lambda_2 H_i^\dagger (\Delta^\dagger)_j^i \Delta_k^j H^k - (\lambda_3 H_i^\dagger \Delta_j^i \Delta_k^j H^k + \lambda_4 S H_i^\dagger \Delta_j^i H^j + \text{H.c.}) + (\text{irrelevant terms}). \quad (4)$$

H^i denotes the SM Higgs doublet, and $H_i^\dagger = (H^i)^\dagger$. The superscripts and subscripts of SU(2) tensors are related by 2-dimensional Levi-Civita symbols ϵ^{ij} and ϵ_{ij} , e.g., $H^i = \epsilon^{ij} H_j$ and $H_i = \epsilon_{ij} H^j$. The omitted terms in $V(S, \Delta)$ are interaction terms among the S and Δ fields, which are irrelevant to the discussions in this work. The EW gauge interaction terms from the covariant derivatives can be found in Ref. [90].

Note that $(\Delta^\dagger)_i^j \Delta_j^i H_k^\dagger H^k$ can be expressed as a linear combination of $H_i^\dagger \Delta_j^i (\Delta^\dagger)_k^j H^k$ and $H_i^\dagger (\Delta^\dagger)_j^i \Delta_k^j H^k$, while $\Delta_j^i \Delta_i^j H_k^\dagger H^k = 2H_i^\dagger \Delta_j^i \Delta_k^j H^k$. Thus, we have listed all independent, renormalizable terms in $V(S, \Delta)$ above. We further assume CP conservation in the scalar sector, and all the parameters in $V(S, \Delta)$ are real.

After the Higgs field $H^i(x)$ gains a nonzero vacuum expectation value v , the interaction terms among the scalar fields contribute to the mass terms of S and Δ . In the unitary gauge, we have $H^1(x) = 0$ and $H^2(x) = [v + h(x)]/\sqrt{2}$. The resulting mass terms of the NP scalars are given by

$$\mathcal{L}_M = -\frac{1}{2} m_a^2 a^2 - \frac{1}{2} \begin{pmatrix} S & \phi \end{pmatrix} M_0^2 \begin{pmatrix} S \\ \phi \end{pmatrix} - \begin{pmatrix} (\Delta^+)^\dagger & \Delta^- \end{pmatrix} M_C^2 \begin{pmatrix} \Delta^+ \\ (\Delta^-)^\dagger \end{pmatrix}, \quad (5)$$

where $m_a^2 = m_\Delta^2 - \mu_\Delta^2 + (\lambda_+ + 2\lambda_3)v^2/4$, and the mass-squared matrices are

$$M_0^2 = \begin{pmatrix} m_S^2 + \lambda_{Sh}v^2/2 & -\lambda_4 v^2/2 \\ -\lambda_4 v^2/2 & m_\Delta^2 + \mu_\Delta^2 + (\lambda_+ - 2\lambda_3)v^2/4 \end{pmatrix}, \quad (6)$$

$$M_C^2 = \begin{pmatrix} m_\Delta^2 + (\lambda_+ - \lambda_-)v^2/4 & \mu_\Delta^2 - \lambda_3 v^2/2 \\ \mu_\Delta^2 - \lambda_3 v^2/2 & m_\Delta^2 + (\lambda_+ + \lambda_-)v^2/4 \end{pmatrix}. \quad (7)$$

Here we have defined $\lambda_\pm \equiv \lambda_1 \pm \lambda_2$.

M_0^2 and M_C^2 can be diagonalized by orthogonal matrices O_0 and O_C , parametrized as

$$O_0 = \begin{pmatrix} c_\beta & -s_\beta \\ s_\beta & c_\beta \end{pmatrix}, \quad O_C = \begin{pmatrix} c_\theta & -s_\theta \\ s_\theta & c_\theta \end{pmatrix}, \quad (8)$$

where the shorthand notations $s_\beta \equiv \sin \beta$ and $c_\beta \equiv \cos \beta$ are used. Then we have

$$O_0^T M_0^2 O_0 = \begin{pmatrix} \mu_1^2 & \\ & \mu_2^2 \end{pmatrix}, \quad O_C^T M_C^2 O_C = \begin{pmatrix} m_1^2 & \\ & m_2^2 \end{pmatrix}, \quad (9)$$

with

$$\mu_{1,2}^2 = \frac{1}{2} \left[m_S^2 + m_\Delta^2 + \mu_\Delta^2 + \frac{1}{4} (2\lambda_{Sh} + \lambda_+ - 2\lambda_3)v^2 \mp \sqrt{r} \right], \quad (10)$$

$$r \equiv \left[m_S^2 - m_\Delta^2 - \mu_\Delta^2 - \frac{1}{4} (\lambda_+ - 2\lambda_3 - 2\lambda_{Sh})v^2 \right]^2 + \lambda_4^2 v^4, \quad (11)$$

$$m_{1,2}^2 = m_\Delta^2 + \frac{v^2}{4} \left[\lambda_+ \mp \sqrt{\lambda_-^2 + 4 \left(\frac{2\mu_\Delta^2}{v^2} - \lambda_3 \right)^2} \right]. \quad (12)$$

The mass hierarchy $\mu_1 \leq \mu_2$ and $m_1 \leq m_2$ is adopted. The rotation angles β and θ are determined by

$$\sin \beta = \frac{-(M_0^2)_{12}}{\sqrt{(M_0^2)_{12}^2 + [(M_0^2)_{11} - \mu_2^2]^2}}, \quad \sin \theta = \frac{-(M_C^2)_{12}}{\sqrt{(M_C^2)_{12}^2 + [(M_C^2)_{11} - m_2^2]^2}}. \quad (13)$$

The neutral mass eigenstates X_i and the charged mass eigenstates Δ_i^\pm are defined by

$$\begin{pmatrix} S \\ \phi \end{pmatrix} = O_0 \begin{pmatrix} X_1 \\ X_2 \end{pmatrix}, \quad \begin{pmatrix} \Delta^+ \\ (\Delta^-)^\dagger \end{pmatrix} = O_C \begin{pmatrix} \Delta_1^+ \\ \Delta_2^+ \end{pmatrix}. \quad (14)$$

Expressing with the mass eigenstates, the mass terms become

$$\mathcal{L}_M = -\frac{1}{2} m_a^2 a^2 - \frac{1}{2} \sum_{i=1}^2 \mu_i^2 X_i^2 - \sum_{i=1}^2 m_i^2 \Delta_i^- \Delta_i^+, \quad (15)$$

where $\Delta_i^- \equiv (\Delta_i^+)^\dagger$.

Now we have one CP -odd neutral scalar boson a , two CP -even neutral scalar bosons X_1 and X_2 , and two singly charged scalar bosons Δ_1^+ and Δ_2^+ accompanied with the antiparticles. They are all Z_2 -odd, and the lightest one is stable, ensured by the Z_2 symmetry. There are eight free parameters in the model, m_S^2 , m_Δ^2 , μ_Δ^2 , λ_{Sh} , λ_+ , λ_- , λ_3 , and λ_4 . It can be proved that $m_a \geq m_1$. Only if $\lambda_- = 0$ and $2\mu_\Delta^2/v^2 - \lambda_3 \geq 0$, we have $m_a = m_1$, otherwise a is heavier than Δ_1^\pm and cannot be a DM candidate. Hereafter we assume that X_1 is the lightest NP scalar, i.e., $\mu_1 < m_a$ and $\mu_1 < m_1$. Thus, the DM candidate in this model is X_1 , whose mass is μ_1 .

The NP corrections to M_W can be given in terms of the EW oblique parameters S , T , and U as [118]

$$\Delta M_W = -\frac{\alpha M_W^{\text{SM}}}{4(c_W^2 - s_W^2)} \left(S - 2c_W^2 T - \frac{c_W^2 - s_W^2}{2s_W^2} U \right) \simeq 0.44 (T - 0.64 S + 0.80 U) \text{ GeV}, \quad (16)$$

where $s_W \equiv \sin \theta_W$, $c_W \equiv \cos \theta_W$, and θ_W is the Weinberg angle. M_W^{SM} is the SM prediction of the W boson mass including radiation corrections. The SM corresponds to the case with $S = T = U = 0$. Denoting $\Pi_{ij}(p^2)$ to be the NP contributions to the $g_{\mu\nu}$ coefficients of the vacuum polarizations of EW gauge bosons i and j , the oblique parameters are defined by [84, 85]

$$S \equiv 16\pi[\Pi'_{33}(0) - \Pi'_{3Q}(0)] = \frac{16\pi s_W^2 c_W^2}{e^2} \left[\Pi'_{ZZ}(0) - \frac{c_W^2 - s_W^2}{s_W c_W} \Pi'_{ZA}(0) - \Pi'_{AA}(0) \right], \quad (17)$$

$$T \equiv \frac{4\pi}{s_W^2 c_W^2 M_Z^2} [\Pi_{11}(0) - \Pi_{33}(0)] = \frac{4\pi}{e^2} \left[\frac{\Pi_{WW}(0)}{M_W^2} - \frac{\Pi_{ZZ}(0)}{M_Z^2} \right], \quad (18)$$

$$U \equiv 16\pi[\Pi'_{11}(0) - \Pi'_{33}(0)] = \frac{16\pi s_W^2}{e^2} [\Pi'_{WW}(0) - c_W^2 \Pi'_{ZZ}(0) - 2s_W c_W \Pi'_{ZA}(0) - s_W^2 \Pi'_{AA}(0)], \quad (19)$$

where $\Pi'_{ij}(0) \equiv \partial\Pi_{ij}(p^2)/\partial p^2|_{p^2=0}$ and e is the electric charge.

Because of EW gauge interactions and mass mixings from spontaneous symmetry breaking, the NP scalars contribute to the self-energies of EW gauge bosons, leading to [90]

$$\begin{aligned} \Pi_{11}(p^2) = \frac{1}{16\pi^2} \{ & 2(1 - s_{2\theta})B_{00}(p^2, m_a^2, m_1^2) + 2(1 + s_{2\theta})B_{00}(p^2, m_a^2, m_2^2) \\ & + 2(1 + s_{2\theta})[s_\beta^2 B_{00}(p^2, \mu_1^2, m_1^2) + c_\beta^2 B_{00}(p^2, \mu_2^2, m_1^2)] \\ & + 2(1 - s_{2\theta})[s_\beta^2 B_{00}(p^2, \mu_1^2, m_2^2) + c_\beta^2 B_{00}(p^2, \mu_2^2, m_2^2)] \\ & - [A_0(m_1^2) + A_0(m_2^2) + A_0(m_a^2) + s_\beta^2 A_0(\mu_1^2) + c_\beta^2 A_0(\mu_2^2)] \}, \end{aligned} \quad (20)$$

$$\Pi_{3Q}(p^2) = \Pi_{33}(p^2) = \frac{1}{16\pi^2} [4B_{00}(p^2, m_1^2, m_1^2) + 4B_{00}(p^2, m_2^2, m_2^2) - 2A_0(m_1^2) - 2A_0(m_2^2)], \quad (21)$$

where A_0 and B_{00} are the standard Passiano-Veltman scalar functions [119]. From these expressions, one can compute the EW oblique parameters. Because of $2B_{00}(0, m^2, m^2) = A_0(m^2)$, we have $\Pi_{3Q}(0) = \Pi_{33}(0) = 0$ and hence $T = 4\pi\Pi_{11}(0)/(s_W^2 c_W^2 M_Z^2)$. The S parameter is related to the hypercharge gauge field by definition. Since neither the singlet nor the triplet carries hypercharge, $\Pi_{3Q}(p^2) = \Pi_{33}(p^2)$ always holds, resulting in $S = 0$ in this model. On the other hand, the T and U parameters would vanish when the custodial symmetry is respected [85, 120]. The condition for the custodial symmetry in the model is $\lambda_- = \lambda_4 = 0$ [90].

Expressing the trilinear interaction term between X_1 and the Higgs boson h as $\mathcal{L}_{hX_1^2} = \lambda_{hX_1^2} v h X_1^2/2$, the dimensionless hX_1^2 coupling is

$$\lambda_{hX_1^2} = -\lambda_{Sh} c_\beta^2 - \frac{1}{2}(\lambda_+ - 2\lambda_3) s_\beta^2 + 2\lambda_4 s_\beta c_\beta. \quad (22)$$

This coupling induces a spin-independent (SI) X_1 -nucleon scattering cross section of [121]

$$\sigma_N^{\text{SI}} = \frac{m_N^2 F_N^2}{4\pi(\mu_1 + m_N)^2}, \quad (23)$$

with

$$F_N = -\frac{\lambda_{hX_1^2} m_N}{9m_h^2} [2 + 7(f_u^N + f_d^N + f_s^N)], \quad (24)$$

where f_q^N are nucleon form factors.

B. Results

In this section, we perform a random scan in the 8-dimensional parameter space of the STSDM model within the following ranges:

$$(10 \text{ GeV})^2 < |m_S^2|, |m_\Delta^2|, |\mu_\Delta^2| < (1 \text{ TeV})^2, \quad 0.001 < |\lambda_{Sh}|, |\lambda_+|, |\lambda_-|, |\lambda_3|, |\lambda_4| < 1. \quad (25)$$

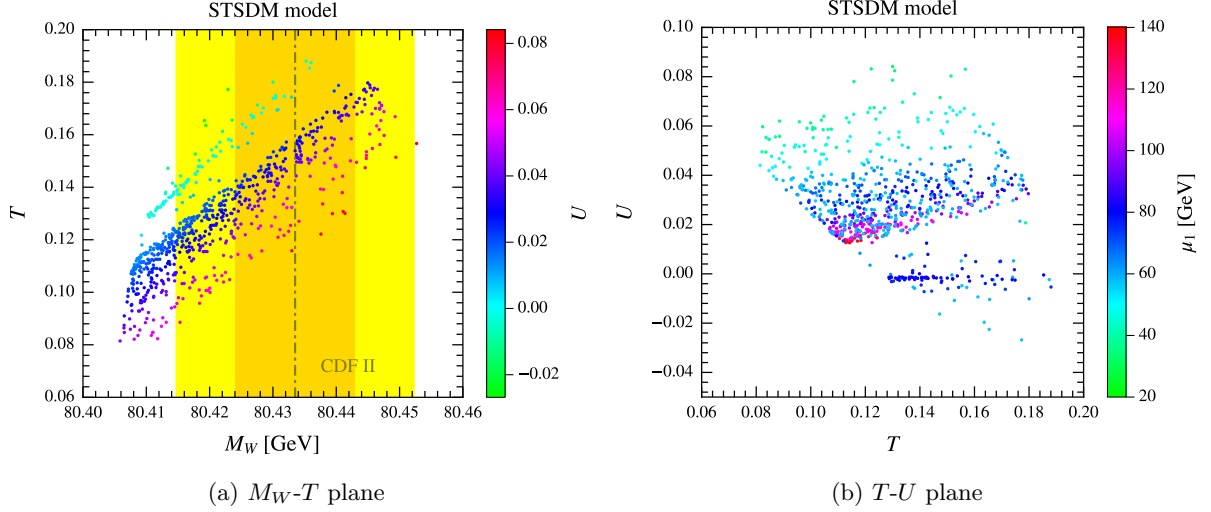


FIG. 1. Selected parameter points projected in the M_W - T (a) and T - U (b) planes for the STSDM model, with the colors corresponding to U and the DM mass μ_1 , respectively. In the left panel, the dot-dashed line denotes the central value of the recent CDF M_W measurement [1], with gold and yellow colors indicating the 1σ and 2σ ranges, respectively.

The EW oblique parameters T and U predicted by each parameter point are calculated based on the above expressions in the help of the code `LoopTools` [122]. We implement the model with `FeynRules` [123, 124] and utilize the package `micrOMEGAs 5.2.13` [125] to compute the X_1 relic density $\Omega_c h^2$, the SI X_1 -nucleon scattering cross section σ_N^{SI} , and the thermally averaged $X_1 X_1$ annihilation cross section today $\langle\sigma v\rangle$.

Firstly, we require the selected parameter points leading to moderate T or U parameters, that can explain the CDF M_W anomaly and satisfy other EW precision tests. Here we adopt the result of a global fit of the oblique parameters to EW precision observables including the recent CDF M_W measurement [10]:

$$S = 0.06 \pm 0.10, \quad T = 0.11 \pm 0.12, \quad U = 0.14 \pm 0.09 \quad (26)$$

with correlation coefficients

$$\rho_{ST} = 0.90, \quad \rho_{SU} = -0.59, \quad \rho_{TU} = -0.85. \quad (27)$$

Note that the fitted S , T , and U are highly correlated, and the correlation coefficients are rather important when evaluating the deviation of the model prediction to the experimental results. The predicted T and U in the STSDM model are required to be within the 95% C.L. region of the fit result, based on a χ^2 calculation. Then we demand the predicted X_1 thermal relic density within the 3σ range of the Planck measurement $\Omega_c h^2 = 0.1200 \pm 0.0012$ [126] and the SI X_1 -nucleon scattering cross section satisfies the constraint from the PandaX-4T direct detection experiment at 90% C.L. [127].

In Fig. 1(a), the selected parameter points projected in the M_W - T plane. Most of the points

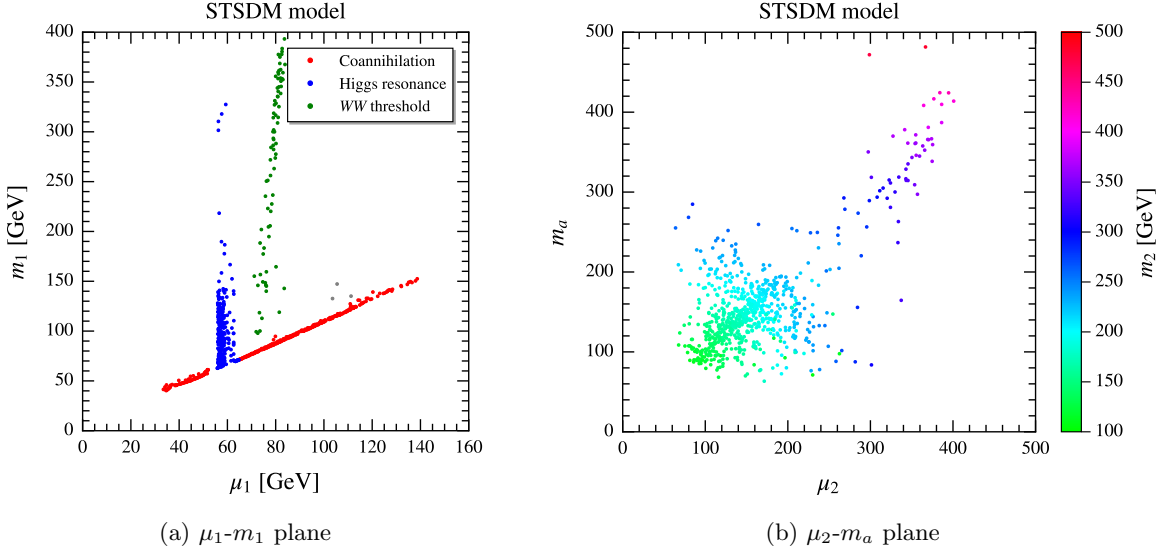


FIG. 2. Selected parameter points projected in the μ_1 - m_1 (a) and μ_2 - m_a (b) planes for the STSDM model. The colors in the left panel indicate three exceptional categories for achieving the correct relic density. The colors in the right panel denotes the Δ_2^\pm mass m_2 .

lie within the 2σ range of the CDF M_W result. The other parameter points are out of the 2σ range but still consistent with the EW global fit at 95% C.L. Figure 1(b) displays the parameter points in the T - U plane with colors indicating the DM mass μ_1 . The allowed region in the T - U plane shows a negative correlation as the fit result of ρ_{TU} implies. A large fraction of the points correspond to $0.07 \lesssim T \lesssim 0.18$ and $0 \lesssim U \lesssim 0.05$. In the framework of effective field theory, T corresponds to a dimension-6 operator $|H^\dagger D_\mu H|^2/\Lambda^2$, while U corresponds to a dimension-8 operator $|H^\dagger W_{\mu\nu}^a \sigma^a H|^2/\Lambda^4$. A large cutoff scale Λ would give more suppression on U than T . Nonetheless, the NP scalars in the loops here have masses around or even below the electroweak scale, so the effective operator description breaks down, and $U \sim T$ can be achieved.

A pure $SU(2)_L$ triplet scalar with EW interactions is expected to give the correct DM relic density for masses around 2 TeV [100]. For interpreting the CDF M_W anomaly, however, the DM candidate X_1 is required to be lighter than 150 GeV, as shown in Fig. 1(b), and X_1 should have a moderate triplet component to contribute to T and U . Current direct detection experiments have strictly constrained the hX_1X_1 coupling $\lambda_{hX_1^2}$ in such a mass range, typically leading to overproduction of the DM relic due to insufficient X_1X_1 annihilation. Nonetheless, it is well known that there are some exceptions for deriving the correct relic density with some special NP mass spectra [128]. If coannihilation, resonant annihilation, or annihilation into forbidden channels has a significant contribution at the freeze-out epoch, then the observed relic density could be achieved for $\mu_1 < 150$ GeV.

In Fig. 2(a), we project the selected parameter points into the μ_1 - m_1 plane, with colors denoting three exceptional categories of points. Firstly, the red points align around the $m_1 = \mu_1$ line would have an important Δ_1^\pm - X_1 coannihilation effect at the freeze-out epoch, because Δ_1^\pm is just a little heavier than X_1 and could effectively annihilate into SM particles. Secondly, the blue points with

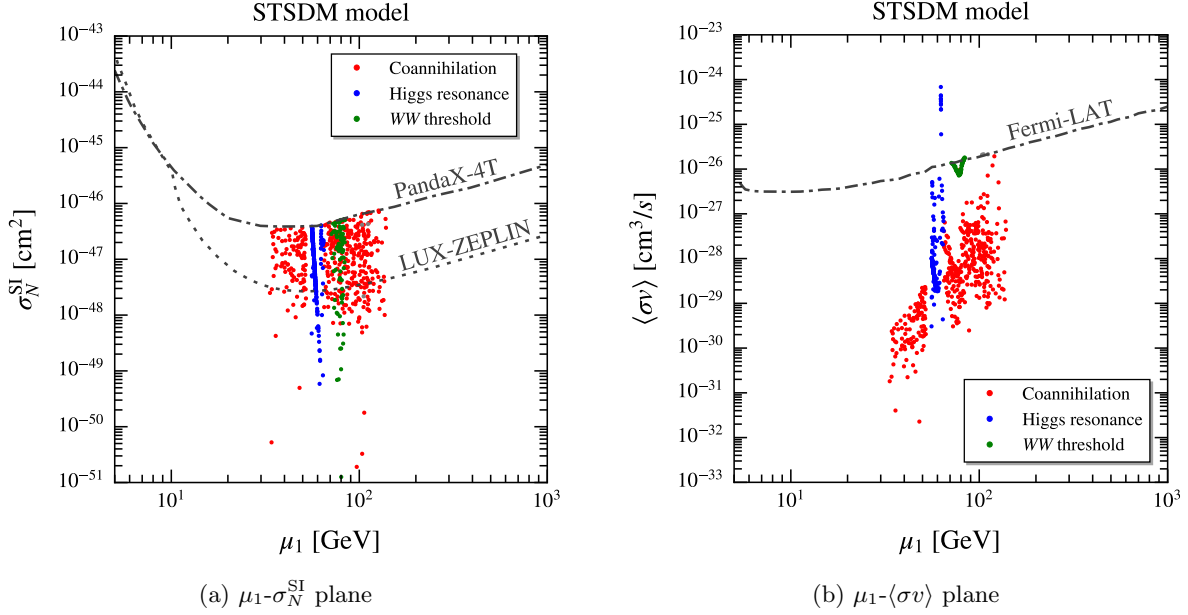


FIG. 3. Selected parameter points projected in the μ_1 - σ_N^{SI} (a) and μ_1 - $\langle\sigma v\rangle$ (b) planes for the STSDM model, with the colors indicating three exceptional categories for achieving the correct relic density. In the left panel, the dot-dashed line denotes the 90% C.L. upper limit from the PandaX-4T direct detection experiment [127], while the dotted line demonstrates the future sensitivity of the LUX-ZEPLIN experiment [129]. The dot-dashed line in the right panel shows the 95% C.L. upper limit for the $b\bar{b}$ annihilation channel from the Fermi-LAT γ -ray observations of dwarf galaxies [130].

$\mu_1 \sim m_h/2$ lead to resonant annihilation of $X_1 X_1$ through a s -channel Higgs boson. Thirdly, the green points with μ_1 slightly smaller than M_W are corresponding to the WW threshold effect. In this case, the 2-body annihilation channel $X_1 X_1 \rightarrow W^+ W^-$ is forbidden today, but opens at the freeze-out epoch due to higher center-of-mass energies at the temperature $\sim \mu_1/25$. Figure 2(b) demonstrates the masses of the a , X_2 , and Δ_2^\pm scalar bosons, which can be as large as 400–500 GeV. But a lot of parameter points correspond to the masses less than 200 GeV.

The SI X_1 -nucleon scattering cross sections corresponding to the selected points are shown in Fig. 3(a). Some parameter points seem far from the reach of the current PandaX-4T direct detection experiment, but a large fraction of them could be properly tested in the future LUX-ZEPLIN experiment [129].

Figure 3(b) displays the total $X_1 X_1$ annihilation cross sections at rest as well as the constraint from the 11-year Fermi-LAT γ -ray observations of 27 dwarf spheroidal galaxies in the $b\bar{b}$ annihilation channel [130]. Most of the points with $\langle\sigma v\rangle$ lower than the standard value $\sim 10^{-26}$ cm^3/s are safe. Note that for the parameter points with μ_1 slightly smaller than M_W , although the 2-body annihilation channel $X_1 X_1 \rightarrow W^+ W^-$ is forbidden today, the 3-body annihilation $X_1 X_1 \rightarrow W^+ W^{*-}$ or $W^{*+} W^-$ could still contribute a moderate $\langle\sigma v\rangle$. A few parameter points with the resonant annihilation have been excluded by the Fermi-LAT search. This is because that for some parameter points with the $X_1 X_1$ annihilation near a very narrow resonance, the annihilation cross section would increase with the decreasing velocities of X_1 . This enhancement could lead to a too

large $\langle\sigma v\rangle$ today.

In order to explain the CDF M_W anomaly, the masses of the NP scalar bosons are required to be smaller than a few hundred GeV. These NP particles could be directly searched at the past and current colliders. If $\mu_1 < m_h/2$, the invisible decay channel $h \rightarrow X_1 X_1$ would open and affect the properties of the 125 GeV Higgs boson. Therefore, we also consider bounds from collider experiments in the scan.

The selected parameter points demonstrated above have also passed the following three tests. First, the signal strengths of the 125 GeV Higgs boson are required to be consistent with current LHC measurements at 95% C.L., based on a global likelihood function constructed by `Lilith 2` [131] implemented in `micrOMEGAs`. Second, we utilize `SModelS 2` [132] interfaced by `micrOMEGAs` to test the parameter points according to the exclusion limits from LHC direct searches for pair production of the NP scalars. Third, we simulate the monojet signature induced by the STSDM model at the 13 TeV LHC with the Monte Carlo generator `MadGraph5_aMC@NLO` [133], and reinterpret the ATLAS monojet analysis for an integrated luminosity of 139 fb^{-1} at $\sqrt{s} = 13 \text{ TeV}$ [134] to set 95% C.L. exclusion limits on the parameter points. We find that the monojet search has excluded the DM candidate mass μ_1 up to $\sim 33 \text{ GeV}$.

In addition, the charged scalars $\Delta_{1,2}^\pm$ could be directly produced in pairs at LEP. A similar search for the lightest chargino by the DELPHI collaboration has excluded the chargino mass up to 103.4 GeV [135]. Thus, we expect that the parameter points with $m_{1,2} \lesssim 100 \text{ GeV}$ might be already excluded. However, such a bound could be relieved if the mass splitting between Δ_1^\pm and X_1 is rather small. Therefore, the constraint on the coannihilation category should be weaker, and a considerable number of the selected parameter points should be free from the LEP and LHC bounds.

III. THE SDFDM MODEL

A. Model

The SDFDM model contains a left-handed Weyl singlet S and two left-handed Weyl doublets D_1 and D_2 with opposite hypercharges. They live in the following $\text{SU}(2)_L \times \text{U}(1)_Y$ representations:

$$S \in (\mathbf{1}, 0), \quad D_1 = \begin{pmatrix} D_1^0 \\ D_1^- \end{pmatrix} \in (\mathbf{2}, -1/2), \quad D_2 = \begin{pmatrix} D_2^+ \\ D_2^0 \end{pmatrix} \in (\mathbf{2}, 1/2). \quad (28)$$

Here D_1^0 and D_2^0 are electrically neutral components, while D_1^- and D_2^+ are singly charged components. The gauge-invariant Lagrangian for the NP sector reads

$$\begin{aligned} \mathcal{L}_{\text{NP}} = & iS^\dagger \bar{\sigma}^\mu \partial_\mu S - \frac{1}{2}(m_S S S + \text{H.c.}) + iD_1^\dagger \bar{\sigma}^\mu D_\mu D_1 + iD_2^\dagger \bar{\sigma}^\mu D_\mu D_2 - (m_D \epsilon_{ij} D_1^i D_2^j + \text{H.c.}) \\ & +(y_1 S D_1^i H_i - y_2 S D_2^i H_i^\dagger + \text{H.c.}), \end{aligned} \quad (29)$$

where the covariant derivative for D_1 and D_2 is $D_\mu = \partial_\mu - igW_\mu^a \sigma_a/2 - ig'YB_\mu$. Assuming CP conservation in the NP sector, the model have four real parameters, including two mass parameters m_S and m_D , and two Yukawa couplings y_1 and y_2 . Without loss of generality, we allow y_1 and y_2 to be positive or negative, while fix $m_S, m_D > 0$.

As the Higgs field develops a vacuum expectation value v , the Yukawa couplings induce Dirac mass terms for the NP fermions. Consequently, the fermion mass terms are given by

$$\mathcal{L}_M = -\frac{1}{2} \begin{pmatrix} S & D_1^0 & D_2^0 \end{pmatrix} M_N \begin{pmatrix} S \\ D_1^0 \\ D_2^0 \end{pmatrix} - m_D D_1^- D_2^+ + \text{H.c.}, \quad (30)$$

where the mass matrix for the neutral fermions is

$$M_N = \begin{pmatrix} m_S & y_1 v/\sqrt{2} & y_2 v/\sqrt{2} \\ y_1 v/\sqrt{2} & 0 & -m_D \\ y_2 v/\sqrt{2} & -m_D & 0 \end{pmatrix}. \quad (31)$$

This matrix can be diagonalized by an orthogonal matrix N , i.e., $N^T M_N N = \text{diag}(m_{\chi_1^0}, m_{\chi_2^0}, m_{\chi_3^0})$. Here we adopt a mass hierarchy of $m_{\chi_1^0} \leq m_{\chi_2^0} \leq m_{\chi_3^0}$.

Defining three neutral mass eigenstates χ_i^0 by

$$\begin{pmatrix} \chi_1^0 \\ \chi_2^0 \\ \chi_3^0 \end{pmatrix} = N^T \begin{pmatrix} S \\ D_1^0 \\ D_2^0 \end{pmatrix}, \quad (32)$$

the mass terms are expressed as

$$\mathcal{L}_M = -\frac{1}{2} \sum_{i=1}^3 m_{\chi_i^0} \chi_i^0 \chi_i^0 - m_{\chi^\pm} \chi^- \chi^+ + \text{H.c.}, \quad (33)$$

with $m_{\chi^\pm} = m_D$, $\chi^+ = D_2^+$, and $\chi^- = D_1^-$. Now we have three Majorana fermions χ_i^0 and two singly charged fermions χ^\pm . Assuming a Z_2 symmetry, the lightest Majorana fermions χ_1^0 can act as a DM candidate. The full Lagrangian describing the interactions between these NP fermions and the SM particles, including the EW gauge bosons and the Higgs boson, can be found in Refs. [89, 93]. These interactions would affect M_W and other EW precision observables via loop corrections. The detailed expressions of $\Pi_{WW}(p^2)$, $\Pi_{ZZ}(p^2)$, $\Pi_{ZA}(p^2)$, and $\Pi_{AA}(p^2)$ contributed by the NP fermions in the SDFDM model are provided in Ref. [89]. Once the fermion masses and couplings to the EW gauge bosons are given as inputs, we can obtain the numerical values of the oblique parameters.

The current results of DM direct detection set stringent constraints on the parameter space of the SDFDM model [89, 93]. The Yukawa couplings give rise to the coupling $g_{h\chi_1^0\chi_1^0}$ between χ_1^0 and the Higgs boson h . This coupling leads to the SI DM-nucleon scattering with a cross section

of [136]

$$\sigma_N^{\text{SI}} = \frac{4\mu_{\chi N}^2 G_{\text{S},N}^2}{\pi}, \quad (34)$$

where $\mu_{\chi N} \equiv m_{\chi_1^0} m_N / (m_{\chi_1^0} + m_N)$ is the DM-nucleon reduced mass, and

$$G_{\text{S},N} = \frac{N_{11} m_N}{9\sqrt{2} v M_h^2} (y_1 N_{21} + y_2 N_{31}) [2 + 7(f_u^N + f_d^N + f_s^N)] \quad (35)$$

is the scalar-type effective coupling. The χ_1^0 coupling to the Z boson $g_{Z\chi_1^0\chi_1^0}$ from the EW gauge interaction also induces a spin-dependent (SD) DM-nucleon scattering cross section [136]

$$\sigma_N^{\text{SD}} = \frac{12}{\pi} \mu_{\chi N}^2 G_{\text{A},N}^2, \quad (36)$$

where the axial-vector effective coupling is

$$G_{\text{A},N} = \sum_{q=u,d,s} \frac{g_A^q g^2 \Delta_q^N}{8c_W^2 M_Z^2} (|N_{31}|^2 - N_{21}^2), \quad (37)$$

where $g_A^u = 1/2$, $g_A^d = g_A^s = -1/2$, and Δ_q^N are the corresponding form factors for the nucleon $N = p, n$.

B. Results

We perform a parameter scan in the 4-dimensional parameter space of the SDFDM model within the following ranges:

$$10 \text{ GeV} < m_S, m_D < 1 \text{ TeV}, \quad -2 < y_1, y_2 < 2. \quad (38)$$

The experimental requirements are the same as those in Sec. II B, except that the constraints from direct detection experiments on the SD scattering are also considered. Here we adopt the the 90% C.L. upper limit on σ_p^{SD} from PICO-60 [137] and that on σ_n^{SI} from PandaX-4T [127]. However, we do not find any viable parameter point that can simultaneously explain the CDF M_W anomaly and the correct DM relic density and avoid the direct detection constraints. This result can be understood as follows.

Let us consider some typical parameter regions, where the stringent constraints from direct detection experiments are avoided. In order to escape from the SI constraint, some specific conditions leading to $g_{h\chi_1^0\chi_1^0} = 0$ have been discussed in Ref. [93]. According to the low energy Higgs theorem [138], we can read $g_{h\chi_1^0\chi_1^0} = \partial m_{\chi_1^0}(v)/\partial v$ from the Lagrangian

$$\mathcal{L}_{h\chi_1^0\chi_1^0} = \frac{1}{2} m_{\chi_1^0}(v) \chi_1^0 \chi_1^0 + \frac{1}{2} \frac{\partial m_{\chi_1^0}(v)}{\partial v} h \chi_1^0 \chi_1^0 + \mathcal{O}(h^2). \quad (39)$$

$m_{\chi_1^0}(v)$ is determined by the characteristic equation $\det(M_N - m_{\chi_1^0}\mathbf{I}) = 0$, which is equivalent to

$$m_{\chi_1^0}^3 - m_S m_{\chi_1^0}^2 - \frac{1}{2}(2m_D^2 + y_1^2 v^2 + y_2^2 v^2)m_{\chi_1^0} + m_D(m_D m_S + y_1 y_2 v^2) = 0. \quad (40)$$

Differentiating this equation and requiring $g_{h\chi_1^0\chi_1^0} = \partial m_{\chi_1^0}(v)/\partial v = 0$, we get

$$m_{\chi_1^0} = \frac{2y_1 y_2 m_D}{y_1^2 + y_2^2}. \quad (41)$$

Applying this result in Eq. (40), we obtain a condition $y_1 = y_2$ for $m_S > m_D > 0$, and another condition

$$y_1 = \frac{y_2}{m_S} \left(m_D \pm \sqrt{m_D^2 - m_S^2} \right) \quad (42)$$

for $m_D > m_S > 0$.

For $m_S > m_D > 0$, the condition $y_1 = y_2$ leads to $m_{\chi_1^0} = m_D$ and $g_{h\chi_1^0\chi_1^0} = 0$. This is the case in the custodial symmetry limit as discussed in Ref. [89]. We can define two $SU(2)_R$ doublets,

$$(\mathcal{D}^A)^i = \begin{pmatrix} D_1^i \\ D_2^i \end{pmatrix}, \quad (\mathcal{H}^A)_i = \begin{pmatrix} H_i^\dagger \\ H_i \end{pmatrix}, \quad (43)$$

and rewrite the Lagrangian of the NP sector with $y_1 = y_2 = y$ as

$$\mathcal{L}_{\text{NP}} = i\mathcal{D}_A^\dagger \bar{\sigma}^\mu D_\mu \mathcal{D}^A - \frac{1}{2}m_D \epsilon_{AB} \epsilon_{ij} (\mathcal{D}^A)^i (\mathcal{D}^B)^j + y \epsilon_{AB} (\mathcal{H}^A)_i S (\mathcal{D}^B)^i + \text{H.c.}, \quad (44)$$

which is invariant under a global $SU(2)_L \times SU(2)_R$ symmetry. In this custodial symmetry limit, χ_1^0 have equal components from the two doublets with opposite hypercharges, resulting in a vanishing $Z\chi_1^0\chi_1^0$ coupling and hence vanishing SD scattering cross sections. Therefore, all the constraints from direct detection are evaded. However, when $y_1 = y_2$, the T and U parameters exactly vanish due to the custodial symmetry [85]. As a result, the parameter points with $y_1 \sim y_2$ cannot induce a large T or U parameter, which is required for explaining the CDF M_W anomaly.

In Fig. 4, we show the parameter points in the y_1 - y_2 plane accounting for the M_W anomaly, and do not find points in the region with $y_1 \sim y_2$. There is also no point with $y_1 \sim -y_2$, due to another custodial symmetry limit $y_1 = -y_2$, which is corresponding to the $SU(2)_R$ doublet defined by $(\mathcal{H}^A)_i = (-H_i^\dagger, H_i)$ instead. In this limit, we also have $T = U = 0$ and $g_{Z\chi_1^0\chi_1^0} = 0$.

For $m_D > m_S > 0$, the condition $y_1/y_2 = (m_D \pm \sqrt{m_D^2 - m_S^2})/m_S$ leads to $m_{\chi_1^0} = m_S$ and $g_{h\chi_1^0\chi_1^0} = 0$. For small y_1 and y_2 , χ_1^0 is dominated by the singlet component. The correct DM relic density could be derived for relatively large y_1 and y_2 , which lead to moderate doublet components in χ_1^0 . However, increasing the doublet components would lift up the $Z\chi_1^0\chi_1^0$ coupling, more easily to be excluded by the SD direct detection constraints. We fix $y_1 = y_2(m_D \pm \sqrt{m_D^2 - m_S^2})/m_S$ and perform a scan with three free parameters, m_S , m_D , and y_2 . No point satisfying all the experimental requirements is found in this scan.

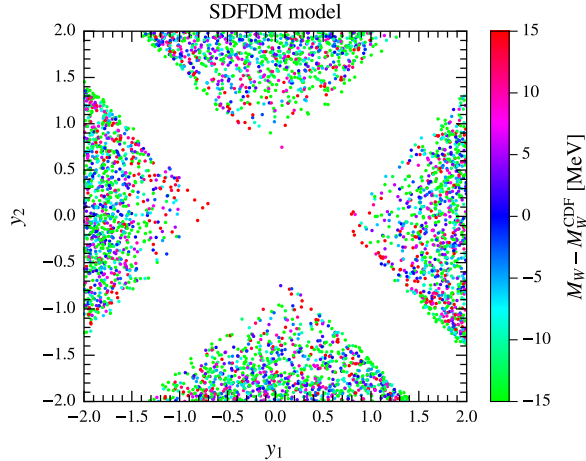


FIG. 4. Parameter points accounting for the CDF M_W anomaly projected in the y_1 - y_2 plane for the SDFDM model. The colors indicate the difference between the predicted M_W and the central value of the CDF measurement M_W^{CDF} . Note that these parameter points are not required to satisfy the DM relic density and direct detection constraints.

The direct detection constraints become rather weak or even vanish when the DM particle mass is below a few GeV, due to the kinematic thresholds in the experiments. It can be observed that Eq. (40) has a solution of $m_{\chi_1^0} = 0$ for $y_1 = -m_D m_S / (y_2 v^2)$. Therefore, for $y_1 \sim -m_D m_S / (y_2 v^2)$, very light χ_1^0 with $m_{\chi_1^0} \sim \mathcal{O}(1)$ GeV could evade the constraints from direct detection experiments. There could be a large splitting in the mass spectrum of the NP fermions, which is useful for generating large oblique parameters. If we only impose the requirements of the M_W anomaly and the direct detection constraints, all the parameter points allowed in the scan correspond to small $m_{\chi_1^0}$. However, since $m_{\chi_1^0}$ is too small, the $\chi_1^0 \chi_1^0$ annihilation channels are rather limited, leading to highly suppressed annihilation cross sections and overproduction of dark matter at the freeze-out epoch. This can be seen in Fig. 5, where the parameter points accounting for the M_W anomaly are shown in the $m_{\chi_1^0}$ - σ_N^{SI} and $m_{\chi_1^0}$ - σ_p^{SD} planes, compared with the direct detection upper limits. The parameter points with very small $m_{\chi_1^0}$ allowed by the direct detection constraints generally predict a large relic density, and no parameter point satisfy the relic density observation.

IV. CONCLUSIONS

In this paper, we study the interpretation of the recent CDF M_W anomaly in the DM models involving extra EW multiplets. We consider both the STSDM and SDFDM models, where new scalar and fermionic multiplets are introduced, respectively. It is obvious that these extra EW multiplets would affect the W boson mass and other EW precision observables through loop corrections. We perform numerical scans in the parameter space of the two models, and attempt to find the parameter points that can simultaneously explain the CDF M_W anomaly and satisfy other EW precision tests and the DM constraints.

In order to generate the measured M_W deviation from the SM prediction, there should be some moderate EW oblique parameters contributed by the NP particles. If such contributions are loop-

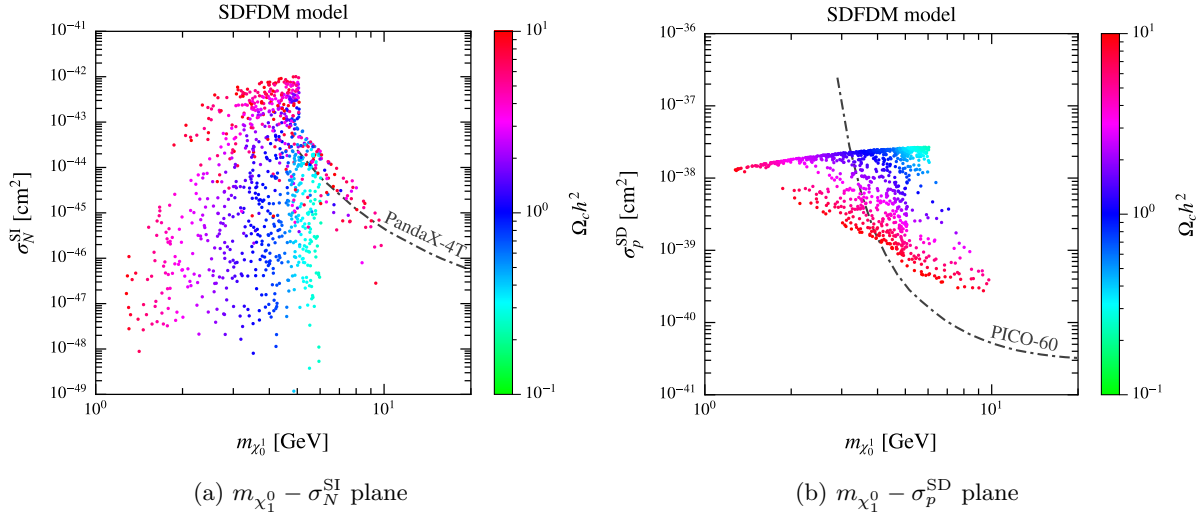


FIG. 5. Parameter points accounting for the CDF M_W anomaly projected in the $m_{\chi_1^0}$ - σ_N^{SI} (a) and $m_{\chi_1^0}$ - σ_p^{SD} (b) planes. The colors indicate the DM thermal relic density. The 90% C.L. upper limit on σ_N^{SI} from the PandaX-4T experiment [127] is indicated in the left panel, while the 90% C.L. upper limit on σ_p^{SD} from the PICO-60 experiment [137] is demonstrated in the right panel. Note that the parameter points leading to the DM-nucleon scattering cross sections much larger than the limits from the direct detection experiments are not shown here.

induced, the corresponding NP particles are required to have masses below a few hundred GeV, and the mass splitting in the NP mass spectrum should be relatively large.

In the STSDM model containing an inert real scalar singlet and an inert complex scalar triplet, we find that many parameter points satisfying all the DM constraints can interpret the CDF M_W anomaly. We observe that the mass range of the DM candidate required by the M_W anomaly is strongly constrained by direct detection experiments, generally leading to small scalar couplings and overproduction of dark matter. In order to avoid this problem, exceptional parameter regions with significant effects of coannihilation, resonantly annihilation, and annihilation to the forbidden channels are typically required to give the correct relic density. Almost all viable parameter points can be classified in these exceptional cases.

In the SDFDM model containing a Weyl singlet and two Weyl doublets, we do not find any parameter point simultaneously satisfying the requirements of the M_W anomaly and DM phenomenology. As a check, we focus on some parameter regions with a vanishing coupling $g_{h\chi_1^0\chi_1}$ or very small $m_{\chi_1^0} \sim \mathcal{O}(1)$ GeV, in order to avoid the stringent constraints from the SI direct detection. We find that the parameter regions with $g_{h\chi_1^0\chi_1} \sim 0$ cannot explain the M_W anomaly or are excluded by the constraints from the SD direct detection, while the parameter regions with small $m_{\chi_1^0}$ cannot give the correct DM relic density. Compared with scalar DM models, fermionic DM models generally have less couplings and less free parameters. Moreover, fermionic DM could also have SD scattering off nucleons in direct detection experiments. These differences make it more difficult for fermionic DM models to simultaneously satisfy all the experimental requirements.

The scenario accounting for the M_W anomaly discussed in this paper can be further tested by future experiments. Since the NP particles interacting with the EW gauge bosons and Higgs

bosons are quite light in this scenario, it is expected that they would have significant production rates at high energy colliders. Furthermore, the NP particles with EW interactions would also modify the production and decay rates of the SM particles via loop corrections. These signatures and effects could be well explored in future collider experiments.

ACKNOWLEDGMENTS

The works of XJB and ZHY are supported by the National Natural Science Foundation of China under Grant Nos. 12175248 and 11805288, respectively. The work of JWW is supported by the research grant “the Dark Universe: A Synergic Multi-messenger Approach” number 2017X7X85K under the program PRIN 2017 funded by the Ministero dell’Istruzione, Università e della Ricerca (MIUR).

-
- [1] **CDF** Collaboration, T. Aaltonen *et al.*, “High-precision measurement of the W boson mass with the CDF II detector,” *Science* **376** (2022) 170–176.
 - [2] **D0** Collaboration, V. M. Abazov *et al.*, “Measurement of the W Boson Mass with the D0 Detector,” *Phys. Rev. Lett.* **108** (2012) 151804, [arXiv:1203.0293 \[hep-ex\]](#).
 - [3] **ATLAS** Collaboration, M. Aaboud *et al.*, “Measurement of the W-boson mass in pp collisions at $\sqrt{s} = 7$ TeV with the ATLAS detector,” *Eur. Phys. J. C* **78** (2018) 110, [arXiv:1701.07240 \[hep-ex\]](#). [Erratum: *Eur.Phys.J.C* 78, 898 (2018)].
 - [4] **LHCb** Collaboration, R. Aaij *et al.*, “Measurement of the W boson mass,” *JHEP* **01** (2022) 036, [arXiv:2109.01113 \[hep-ex\]](#).
 - [5] **CDF** Collaboration, T. Aaltonen *et al.*, “Precise measurement of the W-boson mass with the CDF II detector,” *Phys. Rev. Lett.* **108** (2012) 151803, [arXiv:1203.0275 \[hep-ex\]](#).
 - [6] **Particle Data Group** Collaboration, P. A. Zyla *et al.*, “Review of Particle Physics,” *PTEP* **2020** (2020) 083C01.
 - [7] J. de Blas, M. Ciuchini, E. Franco, A. Goncalves, S. Mishima, M. Pierini, L. Reina, and L. Silvestrini, “Global analysis of electroweak data in the Standard Model,” [arXiv:2112.07274 \[hep-ph\]](#).
 - [8] Y.-Z. Fan, T.-P. Tang, Y.-L. S. Tsai, and L. Wu, “Inert Higgs Dark Matter for New CDF W-boson Mass and Detection Prospects,” [arXiv:2204.03693 \[hep-ph\]](#).
 - [9] C.-R. Zhu, M.-Y. Cui, Z.-Q. Xia, Z.-H. Yu, X. Huang, Q. Yuan, and Y. Z. Fan, “GeV antiproton/gamma-ray excesses and the W-boson mass anomaly: three faces of $\sim 60 - 70$ GeV dark matter particle?,” [arXiv:2204.03767 \[astro-ph.HE\]](#).
 - [10] C.-T. Lu, L. Wu, Y. Wu, and B. Zhu, “Electroweak Precision Fit and New Physics in light of W Boson Mass,” [arXiv:2204.03796 \[hep-ph\]](#).
 - [11] P. Athron, A. Fowlie, C.-T. Lu, L. Wu, Y. Wu, and B. Zhu, “The W boson Mass and Muon $g - 2$: Hadronic Uncertainties or New Physics?,” [arXiv:2204.03996 \[hep-ph\]](#).
 - [12] G.-W. Yuan, L. Zu, L. Feng, and Y.-F. Cai, “W-boson mass anomaly: probing the models of axion-like particle, dark photon and Chameleon dark energy,” [arXiv:2204.04183 \[hep-ph\]](#).
 - [13] A. Strumia, “Interpreting electroweak precision data including the W-mass CDF anomaly,” [arXiv:2204.04191 \[hep-ph\]](#).

- [14] J. M. Yang and Y. Zhang, “Low energy SUSY confronted with new measurements of W-boson mass and muon $g-2$,” [arXiv:2204.04202 \[hep-ph\]](#).
- [15] J. de Blas, M. Pierini, L. Reina, and L. Silvestrini, “Impact of the recent measurements of the top-quark and W-boson masses on electroweak precision fits,” [arXiv:2204.04204 \[hep-ph\]](#).
- [16] X. K. Du, Z. Li, F. Wang, and Y. K. Zhang, “Explaining The Muon $g - 2$ Anomaly and New CDFII W-Boson Mass in the Framework of ExtraOrdinary Gauge Mediation,” [arXiv:2204.04286 \[hep-ph\]](#).
- [17] T.-P. Tang, M. Abdughani, L. Feng, Y.-L. S. Tsai, and Y.-Z. Fan, “NMSSM neutralino dark matter for W-boson mass and muon $g - 2$ and the promising prospect of direct detection,” [arXiv:2204.04356 \[hep-ph\]](#).
- [18] G. Cacciapaglia and F. Sannino, “The W boson mass weighs in on the non-standard Higgs,” [arXiv:2204.04514 \[hep-ph\]](#).
- [19] M. Blennow, P. Coloma, E. Fernández-Martínez, and M. González-López, “Right-handed neutrinos and the CDF II anomaly,” [arXiv:2204.04559 \[hep-ph\]](#).
- [20] F. Arias-Aragón, E. Fernández-Martínez, M. González-López, and L. Merlo, “Dynamical Minimal Flavour Violating Inverse Seesaw,” [arXiv:2204.04672 \[hep-ph\]](#).
- [21] B.-Y. Zhu, S. Li, J.-G. Cheng, R.-L. Li, and Y.-F. Liang, “Using gamma-ray observation of dwarf spheroidal galaxy to test a dark matter model that can interpret the W-boson mass anomaly,” [arXiv:2204.04688 \[astro-ph.HE\]](#).
- [22] K. Sakurai, F. Takahashi, and W. Yin, “Singlet extensions and W boson mass in the light of the CDF II result,” [arXiv:2204.04770 \[hep-ph\]](#).
- [23] J. Fan, L. Li, T. Liu, and K.-F. Lyu, “W-Boson Mass, Electroweak Precision Tests and SMEFT,” [arXiv:2204.04805 \[hep-ph\]](#).
- [24] X. Liu, S.-Y. Guo, B. Zhu, and Y. Li, “Unifying gravitational waves with W boson, FIMP dark matter, and Majorana Seesaw mechanism,” [arXiv:2204.04834 \[hep-ph\]](#).
- [25] H. M. Lee and K. Yamashita, “A Model of Vector-like Leptons for the Muon $g - 2$ and the W Boson Mass,” [arXiv:2204.05024 \[hep-ph\]](#).
- [26] Y. Cheng, X.-G. He, Z.-L. Huang, and M.-W. Li, “Type-II Seesaw Triplet Scalar and Its VEV Effects on Neutrino Trident Scattering and W mass,” [arXiv:2204.05031 \[hep-ph\]](#).
- [27] H. Song, W. Su, and M. Zhang, “Electroweak Phase Transition in 2HDM under Higgs, Z-pole, and W precision measurements,” [arXiv:2204.05085 \[hep-ph\]](#).
- [28] E. Bagnaschi, J. Ellis, M. Madigan, K. Mimasu, V. Sanz, and T. You, “SMEFT Analysis of m_W ,” [arXiv:2204.05260 \[hep-ph\]](#).
- [29] A. Paul and M. Valli, “Violation of custodial symmetry from W-boson mass measurements,” [arXiv:2204.05267 \[hep-ph\]](#).
- [30] H. Bahl, J. Braathen, and G. Weiglein, “New physics effects on the W-boson mass from a doublet extension of the SM Higgs sector,” [arXiv:2204.05269 \[hep-ph\]](#).
- [31] P. Asadi, C. Cesarotti, K. Fraser, S. Homiller, and A. Parikh, “Oblique Lessons from the W Mass Measurement at CDF II,” [arXiv:2204.05283 \[hep-ph\]](#).
- [32] L. Di Luzio, R. Gröber, and P. Paradisi, “Higgs physics confronts the M_W anomaly,” [arXiv:2204.05284 \[hep-ph\]](#).
- [33] P. Athron, M. Bach, D. H. J. Jacob, W. Kotlarski, D. Stöckinger, and A. Voigt, “Precise calculation of the W boson pole mass beyond the Standard Model with FlexibleSUSY,” [arXiv:2204.05285 \[hep-ph\]](#).
- [34] J. Gu, Z. Liu, T. Ma, and J. Shu, “Speculations on the W-Mass Measurement at CDF,” [arXiv:2204.05296 \[hep-ph\]](#).

- [35] J. J. Heckman, “Extra W -Boson Mass from a D3-Brane,” [arXiv:2204.05302 \[hep-ph\]](#).
- [36] K. S. Babu, S. Jana, and V. P. K., “Correlating W -Boson Mass Shift with Muon $g - 2$ in the 2HDM,” [arXiv:2204.05303 \[hep-ph\]](#).
- [37] Y. Heo, D.-W. Jung, and J. S. Lee, “Impact of the CDF W -mass anomaly on two Higgs doublet model,” [arXiv:2204.05728 \[hep-ph\]](#).
- [38] X. K. Du, Z. Li, F. Wang, and Y. K. Zhang, “Explaining The New CDFII W -Boson Mass In The Georgi-Machacek Extension Models,” [arXiv:2204.05760 \[hep-ph\]](#).
- [39] K. Cheung, W.-Y. Keung, and P.-Y. Tseng, “Iso-doublet Vector Leptoquark solution to the Muon $g - 2$, R_{K,K^*} , R_{D,D^*} , and W -mass Anomalies,” [arXiv:2204.05942 \[hep-ph\]](#).
- [40] A. Crivellin, M. Kirk, T. Kitahara, and F. Mescia, “Correlating $t \rightarrow cZ$ to the W Mass and B Physics with Vector-Like Quarks,” [arXiv:2204.05962 \[hep-ph\]](#).
- [41] M. Endo and S. Mishima, “New physics interpretation of W -boson mass anomaly,” [arXiv:2204.05965 \[hep-ph\]](#).
- [42] T. Biekötter, S. Heinemeyer, and G. Weiglein, “Excesses in the low-mass Higgs-boson search and the W -boson mass measurement,” [arXiv:2204.05975 \[hep-ph\]](#).
- [43] R. Balkin, E. Madge, T. Menzo, G. Perez, Y. Soreq, and J. Zupan, “On the implications of positive W mass shift,” [arXiv:2204.05992 \[hep-ph\]](#).
- [44] N. V. Krasnikov, “Nonlocal generalization of the SM as an explanation of recent CDF result,” [arXiv:2204.06327 \[hep-ph\]](#).
- [45] Y. H. Ahn, S. K. Kang, and R. Ramos, “Implications of New CDF-II W Boson Mass on Two Higgs Doublet Model,” [arXiv:2204.06485 \[hep-ph\]](#).
- [46] X.-F. Han, F. Wang, L. Wang, J. M. Yang, and Y. Zhang, “A joint explanation of W -mass and muon $g-2$ in 2HDM,” [arXiv:2204.06505 \[hep-ph\]](#).
- [47] M.-D. Zheng, F.-Z. Chen, and H.-H. Zhang, “The $W\ell\nu$ -vertex corrections to W -boson mass in the R-parity violating MSSM,” [arXiv:2204.06541 \[hep-ph\]](#).
- [48] J. Kawamura, S. Okawa, and Y. Omura, “ W boson mass and muon $g - 2$ in a lepton portal dark matter model,” [arXiv:2204.07022 \[hep-ph\]](#).
- [49] Z. Péli and Z. Trócsányi, “Vacuum stability and scalar masses in the superweak extension of the standard model,” [arXiv:2204.07100 \[hep-ph\]](#).
- [50] A. Ghoshal, N. Okada, S. Okada, D. Raut, Q. Shafi, and A. Thapa, “Type III seesaw with R-parity violation in light of m_W (CDF),” [arXiv:2204.07138 \[hep-ph\]](#).
- [51] P. F. Perez, H. H. Patel, and A. D. Plascencia, “On the W -mass and New Higgs Bosons,” [arXiv:2204.07144 \[hep-ph\]](#).
- [52] S. Kanemura and K. Yagyu, “Implication of the W boson mass anomaly at CDF II in the Higgs triplet model with a mass difference,” [arXiv:2204.07511 \[hep-ph\]](#).
- [53] P. Mondal, “Enhancement of the W boson mass in the Georgi-Machacek model,” [arXiv:2204.07844 \[hep-ph\]](#).
- [54] K.-Y. Zhang and W.-Z. Feng, “Explaining W boson mass anomaly and dark matter with a $U(1)$ dark sector,” [arXiv:2204.08067 \[hep-ph\]](#).
- [55] D. Borah, S. Mahapatra, D. Nanda, and N. Sahu, “Type II Dirac Seesaw with Observable ΔN_{eff} in the light of W -mass Anomaly,” [arXiv:2204.08266 \[hep-ph\]](#).
- [56] T. A. Chowdhury, J. Heeck, S. Saad, and A. Thapa, “ W boson mass shift and muon magnetic moment in the Zee model,” [arXiv:2204.08390 \[hep-ph\]](#).
- [57] G. Arcadi and A. Djouadi, “The 2HD+a model for a combined explanation of the possible excesses in the CDF M_W measurement and $(g - 2)_\mu$ with Dark Matter,” [arXiv:2204.08406 \[hep-ph\]](#).
- [58] V. Cirigliano, W. Dekens, J. de Vries, E. Mereghetti, and T. Tong, “Beta-decay implications for the

- W-boson mass anomaly,” [arXiv:2204.08440 \[hep-ph\]](#).
- [59] L. M. Carpenter, T. Murphy, and M. J. Smylie, “Changing patterns in electroweak precision with new color-charged states: Oblique corrections and the W boson mass,” [arXiv:2204.08546 \[hep-ph\]](#).
- [60] O. Popov and R. Srivastava, “The Triplet Dirac Seesaw in the View of the Recent CDF-II W Mass Anomaly,” [arXiv:2204.08568 \[hep-ph\]](#).
- [61] K. Ghorbani and P. Ghorbani, “ W -Boson Mass Anomaly from Scale Invariant 2HDM,” [arXiv:2204.09001 \[hep-ph\]](#).
- [62] M. Du, Z. Liu, and P. Nath, “CDF W mass anomaly in a Stueckelberg extended standard model,” [arXiv:2204.09024 \[hep-ph\]](#).
- [63] A. Bhaskar, A. A. Madathil, T. Mandal, and S. Mitra, “Combined explanation of W -mass, muon $g - 2$, $R_{K^{(*)}}$ and $R_{D^{(*)}}$ anomalies in a singlet-triplet scalar leptoquark model,” [arXiv:2204.09031 \[hep-ph\]](#).
- [64] A. Batra, S. K. A, S. Mandal, and R. Srivastava, “ W boson mass in Singlet-Triplet Scotogenic dark matter model,” [arXiv:2204.09376 \[hep-ph\]](#).
- [65] J. Cao, L. Meng, L. Shang, S. Wang, and B. Yang, “Interpreting the W mass anomaly in the vectorlike quark models,” [arXiv:2204.09477 \[hep-ph\]](#).
- [66] Y.-P. Zeng, C. Cai, Y.-H. Su, and H.-H. Zhang, “Extra boson mix with Z boson explaining the mass of W boson,” [arXiv:2204.09487 \[hep-ph\]](#).
- [67] S. Baek, “Implications of CDF W -mass and $(g - 2)_\mu$ on $U(1)_{L_\mu - L_\tau}$ model,” [arXiv:2204.09585 \[hep-ph\]](#).
- [68] D. Borah, S. Mahapatra, and N. Sahu, “Singlet-Doublet Fermion Origin of Dark Matter, Neutrino Mass and W -Mass Anomaly,” [arXiv:2204.09671 \[hep-ph\]](#).
- [69] E. d. S. Almeida, A. Alves, O. J. P. Eboli, and M. C. Gonzalez-Garcia, “Impact of CDF-II measurement of M_W on the electroweak legacy of the LHC Run II,” [arXiv:2204.10130 \[hep-ph\]](#).
- [70] Y. Cheng, X.-G. He, F. Huang, J. Sun, and Z.-P. Xing, “Dark photon kinetic mixing effects for CDF W mass excess,” [arXiv:2204.10156 \[hep-ph\]](#).
- [71] J. Heeck, “ W -boson mass in the triplet seesaw model,” [arXiv:2204.10274 \[hep-ph\]](#).
- [72] A. Addazi, A. Marciano, R. Pasechnik, and H. Yang, “CDF II W -mass anomaly faces first-order electroweak phase transition,” [arXiv:2204.10315 \[hep-ph\]](#).
- [73] S. Lee, K. Cheung, J. Kim, C.-T. Lu, and J. Song, “Status of the two-Higgs-doublet model in light of the CDF m_W measurement,” [arXiv:2204.10338 \[hep-ph\]](#).
- [74] C. Cai, D. Qiu, Y.-L. Tang, Z.-H. Yu, and H.-H. Zhang, “Corrections to electroweak precision observables from mixings of an exotic vector boson in light of the CDF W -mass anomaly,” [arXiv:2204.11570 \[hep-ph\]](#).
- [75] R. Benbrik, M. Boukidi, and B. Manaut, “ W -mass and 96 GeV excess in type-III 2HDM,” [arXiv:2204.11755 \[hep-ph\]](#).
- [76] T. Yang, S. Qian, S. Deng, J. Xiao, L. Gao, A. M. Levin, Q. Li, M. Lu, and Z. You, “The physics case for a neutrino lepton collider in light of the CDF W mass measurement,” [arXiv:2204.11871 \[hep-ph\]](#).
- [77] A. Batra, S. K. A, S. Mandal, H. Prajapati, and R. Srivastava, “CDF-II W Boson Mass Anomaly in the Canonical Scotogenic Neutrino-Dark Matter Model,” [arXiv:2204.11945 \[hep-ph\]](#).
- [78] H. B. T. Tan and A. Derevianko, “Implications of W -boson mass for atomic parity violation,” [arXiv:2204.11991 \[hep-ph\]](#).
- [79] H. Abouabid, A. Arhrib, R. Benbrik, M. Krab, and M. Ouchemhou, “Is the new CDF M_W measurement consistent with the two higgs doublet model?,” [arXiv:2204.12018 \[hep-ph\]](#).

- [80] H. Gisbert, V. Miralles, and J. Ruiz-Vidal, “W-boson mass and electric dipole moments from colour-octet scalars,” in *Postponed: 30th International Symposium on Lepton Photon Interactions at High Energies*. 4, 2022, [arXiv:2204.12453 \[hep-ph\]](#).
- [81] T.-K. Chen, C.-W. Chiang, and K. Yagyu, “Explanation of the W mass shift at CDF II in the Georgi-Machacek Model,” [arXiv:2204.12898 \[hep-ph\]](#).
- [82] Q. Zhou and X.-F. Han, “The CDF W -mass, muon $g-2$, and dark matter in a $U(1)_{L_\mu-L_\tau}$ model with vector-like leptons,” [arXiv:2204.13027 \[hep-ph\]](#).
- [83] R. S. Gupta, “Running away from the T-parameter solution to the W mass anomaly,” [arXiv:2204.13690 \[hep-ph\]](#).
- [84] M. E. Peskin and T. Takeuchi, “A New constraint on a strongly interacting Higgs sector,” *Phys. Rev. Lett.* **65** (1990) 964–967.
- [85] M. E. Peskin and T. Takeuchi, “Estimation of oblique electroweak corrections,” *Phys. Rev. D* **46** (1992) 381–409.
- [86] F. D’Eramo, “Dark matter and Higgs boson physics,” *Phys. Rev. D* **76** (2007) 083522, [arXiv:0705.4493 \[hep-ph\]](#).
- [87] A. Dedes and D. Karamitros, “Doublet-Triplet Fermionic Dark Matter,” *Phys. Rev. D* **89** (2014) 115002, [arXiv:1403.7744 \[hep-ph\]](#).
- [88] M. A. Fedderke, T. Lin, and L.-T. Wang, “Probing the fermionic Higgs portal at lepton colliders,” *JHEP* **04** (2016) 160, [arXiv:1506.05465 \[hep-ph\]](#).
- [89] C. Cai, Z.-H. Yu, and H.-H. Zhang, “CEPC Precision of Electroweak Oblique Parameters and Weakly Interacting Dark Matter: the Fermionic Case,” *Nucl. Phys. B* **921** (2017) 181–210, [arXiv:1611.02186 \[hep-ph\]](#).
- [90] C. Cai, Z.-H. Yu, and H.-H. Zhang, “CEPC Precision of Electroweak Oblique Parameters and Weakly Interacting Dark Matter: the Scalar Case,” *Nucl. Phys. B* **924** (2017) 128–152, [arXiv:1705.07921 \[hep-ph\]](#).
- [91] M. McCullough, “An Indirect Model-Dependent Probe of the Higgs Self-Coupling,” *Phys. Rev. D* **90** (2014) 015001, [arXiv:1312.3322 \[hep-ph\]](#). [Erratum: *Phys.Rev.D* 92, 039903 (2015)].
- [92] A. Freitas, S. Westhoff, and J. Zupan, “Integrating in the Higgs Portal to Fermion Dark Matter,” *JHEP* **09** (2015) 015, [arXiv:1506.04149 \[hep-ph\]](#).
- [93] Q.-F. Xiang, X.-J. Bi, P.-F. Yin, and Z.-H. Yu, “Exploring Fermionic Dark Matter via Higgs Boson Precision Measurements at the Circular Electron Positron Collider,” *Phys. Rev. D* **97** (2018) 055004, [arXiv:1707.03094 \[hep-ph\]](#).
- [94] J. Elias-Miro, J. R. Espinosa, G. F. Giudice, H. M. Lee, and A. Strumia, “Stabilization of the Electroweak Vacuum by a Scalar Threshold Effect,” *JHEP* **06** (2012) 031, [arXiv:1203.0237 \[hep-ph\]](#).
- [95] N. Chakrabarty, U. K. Dey, and B. Mukhopadhyaya, “High-scale validity of a two-Higgs doublet scenario: a study including LHC data,” *JHEP* **12** (2014) 166, [arXiv:1407.2145 \[hep-ph\]](#).
- [96] A. Dutta Banik, A. K. Saha, and A. Sil, “Scalar assisted singlet doublet fermion dark matter model and electroweak vacuum stability,” *Phys. Rev. D* **98** (2018) 075013, [arXiv:1806.08080 \[hep-ph\]](#).
- [97] N. Khan, “Exploring the hyperchargeless Higgs triplet model up to the Planck scale,” *Eur. Phys. J. C* **78** (2018) 341, [arXiv:1610.03178 \[hep-ph\]](#).
- [98] J.-W. Wang, X.-J. Bi, P.-F. Yin, and Z.-H. Yu, “Impact of Fermionic Electroweak Multiplet Dark Matter on Vacuum Stability with One-loop Matching,” *Phys. Rev. D* **99** (2019) 055009, [arXiv:1811.08743 \[hep-ph\]](#).
- [99] R. Mahbubani and L. Senatore, “The Minimal model for dark matter and unification,” *Phys. Rev. D* **73** (2006) 043510, [arXiv:hep-ph/0510064](#).

- [100] M. Cirelli, N. Fornengo, and A. Strumia, “Minimal dark matter,” *Nucl. Phys. B* **753** (2006) 178–194, [arXiv:hep-ph/0512090](#).
- [101] R. Enberg, P. J. Fox, L. J. Hall, A. Y. Papaioannou, and M. Papucci, “LHC and dark matter signals of improved naturalness,” *JHEP* **11** (2007) 014, [arXiv:0706.0918 \[hep-ph\]](#).
- [102] T. Cohen, J. Kearney, A. Pierce, and D. Tucker-Smith, “Singlet-Doublet Dark Matter,” *Phys. Rev. D* **85** (2012) 075003, [arXiv:1109.2604 \[hep-ph\]](#).
- [103] C. Cheung and D. Sanford, “Simplified Models of Mixed Dark Matter,” *JCAP* **02** (2014) 011, [arXiv:1311.5896 \[hep-ph\]](#).
- [104] L. Calibbi, A. Mariotti, and P. Tziveloglou, “Singlet-Doublet Model: Dark matter searches and LHC constraints,” *JHEP* **10** (2015) 116, [arXiv:1505.03867 \[hep-ph\]](#).
- [105] C. Cai, Z.-M. Huang, Z. Kang, Z.-H. Yu, and H.-H. Zhang, “Perturbativity Limits for Scalar Minimal Dark Matter with Yukawa Interactions: Septuplet,” *Phys. Rev. D* **92** (2015) 115004, [arXiv:1510.01559 \[hep-ph\]](#).
- [106] T. M. P. Tait and Z.-H. Yu, “Triplet-Quadruplet Dark Matter,” *JHEP* **03** (2016) 204, [arXiv:1601.01354 \[hep-ph\]](#).
- [107] S. Horiuchi, O. Macias, D. Restrepo, A. Rivera, O. Zapata, and H. Silverwood, “The Fermi-LAT gamma-ray excess at the Galactic Center in the singlet-doublet fermion dark matter model,” *JCAP* **03** (2016) 048, [arXiv:1602.04788 \[hep-ph\]](#).
- [108] S. Banerjee, S. Matsumoto, K. Mukaida, and Y.-L. S. Tsai, “WIMP Dark Matter in a Well-Tempered Regime: A case study on Singlet-Doublets Fermionic WIMP,” *JHEP* **11** (2016) 070, [arXiv:1603.07387 \[hep-ph\]](#).
- [109] T. Abe, “Effect of CP violation in the singlet-doublet dark matter model,” *Phys. Lett. B* **771** (2017) 125–130, [arXiv:1702.07236 \[hep-ph\]](#).
- [110] J.-W. Wang, X.-J. Bi, Q.-F. Xiang, P.-F. Yin, and Z.-H. Yu, “Exploring triplet-quadruplet fermionic dark matter at the LHC and future colliders,” *Phys. Rev. D* **97** (2018) 035021, [arXiv:1711.05622 \[hep-ph\]](#).
- [111] Z. Luo, C. Cai, Z. Kang, Z.-H. Yu, and H.-H. Zhang, “Scalar quintuplet minimal dark matter with Yukawa interactions: perturbative up to the Planck scale,” *Chin. Phys. C* **43** (2019) 023102, [arXiv:1711.07396 \[hep-ph\]](#).
- [112] L. Lopez Honorez, M. H. G. Tytgat, P. Tziveloglou, and B. Zaldivar, “On Minimal Dark Matter coupled to the Higgs,” *JHEP* **04** (2018) 011, [arXiv:1711.08619 \[hep-ph\]](#).
- [113] T. Abe and R. Sato, “Current status and future prospects of the singlet-doublet dark matter model with CP-violation,” *Phys. Rev. D* **99** (2019) 035012, [arXiv:1901.02278 \[hep-ph\]](#).
- [114] Y.-P. Zeng, C. Cai, D.-Y. Liu, Z.-H. Yu, and H.-H. Zhang, “Probing quadruplet scalar dark matter at current and future pp colliders,” *Phys. Rev. D* **101** (2020) 115033, [arXiv:1910.09431 \[hep-ph\]](#).
- [115] D.-Y. Liu, C. Cai, Z.-H. Yu, Y.-P. Zeng, and H.-H. Zhang, “Inert sextuplet scalar dark matter at the LHC and future colliders,” *JHEP* **10** (2020) 212, [arXiv:2008.06821 \[hep-ph\]](#).
- [116] K. Fraser, A. Parikh, and W. L. Xu, “A Closer Look at CP-Violating Higgs Portal Dark Matter as a Candidate for the GCE,” *JHEP* **03** (2021) 123, [arXiv:2010.15129 \[hep-ph\]](#).
- [117] L.-Q. Gao, X.-J. Bi, J.-W. Wang, Q.-F. Xiang, and P.-F. Yin, “Exploring Fermionic Multiplet Dark Matter through Precision Measurements at the CEPC,” [arXiv:2112.02519 \[hep-ph\]](#).
- [118] M. Ciuchini, E. Franco, S. Mishima, and L. Silvestrini, “Electroweak Precision Observables, New Physics and the Nature of a 126 GeV Higgs Boson,” *JHEP* **08** (2013) 106, [arXiv:1306.4644 \[hep-ph\]](#).
- [119] G. Passarino and M. J. G. Veltman, “One Loop Corrections for $e^+ e^-$ Annihilation Into $\mu^+ \mu^-$ in the Weinberg Model,” *Nucl. Phys. B* **160** (1979) 151–207.

- [120] P. Sikivie, L. Susskind, M. B. Voloshin, and V. I. Zakharov, “Isospin Breaking in Technicolor Models,” *Nucl. Phys. B* **173** (1980) 189–207.
- [121] Z.-H. Yu, J.-M. Zheng, X.-J. Bi, Z. Li, D.-X. Yao, and H.-H. Zhang, “Constraining the interaction strength between dark matter and visible matter: II. scalar, vector and spin-3/2 dark matter,” *Nucl. Phys. B* **860** (2012) 115–151, [arXiv:1112.6052 \[hep-ph\]](#).
- [122] T. Hahn and M. Perez-Victoria, “Automatized one loop calculations in four-dimensions and D-dimensions,” *Comput. Phys. Commun.* **118** (1999) 153–165, [arXiv:hep-ph/9807565](#).
- [123] N. D. Christensen, P. de Aquino, C. Degrande, C. Duhr, B. Fuks, M. Herquet, F. Maltoni, and S. Schumann, “A Comprehensive approach to new physics simulations,” *Eur. Phys. J. C* **71** (2011) 1541, [arXiv:0906.2474 \[hep-ph\]](#).
- [124] A. Alloul, N. D. Christensen, C. Degrande, C. Duhr, and B. Fuks, “FeynRules 2.0 - A complete toolbox for tree-level phenomenology,” *Comput. Phys. Commun.* **185** (2014) 2250–2300, [arXiv:1310.1921 \[hep-ph\]](#).
- [125] G. Belanger, A. Mjallal, and A. Pukhov, “Recasting direct detection limits within micrOMEGAs and implication for non-standard Dark Matter scenarios,” *Eur. Phys. J. C* **81** (2021) 239, [arXiv:2003.08621 \[hep-ph\]](#).
- [126] **Planck** Collaboration, N. Aghanim *et al.*, “Planck 2018 results. VI. Cosmological parameters,” *Astron. Astrophys.* **641** (2020) A6, [arXiv:1807.06209 \[astro-ph.CO\]](#). [Erratum: *Astron. Astrophys.* 652, C4 (2021)].
- [127] **PandaX-4T** Collaboration, Y. Meng *et al.*, “Dark Matter Search Results from the PandaX-4T Commissioning Run,” *Phys. Rev. Lett.* **127** (2021) 261802, [arXiv:2107.13438 \[hep-ex\]](#).
- [128] K. Griest and D. Seckel, “Three exceptions in the calculation of relic abundances,” *Phys. Rev. D* **43** (1991) 3191–3203.
- [129] B. J. Mount *et al.*, “LUX-ZEPLIN (LZ) Technical Design Report,” [arXiv:1703.09144 \[physics.ins-det\]](#).
- [130] S. Hoof, A. Geringer-Sameth, and R. Trotta, “A Global Analysis of Dark Matter Signals from 27 Dwarf Spheroidal Galaxies using 11 Years of Fermi-LAT Observations,” *JCAP* **02** (2020) 012, [arXiv:1812.06986 \[astro-ph.CO\]](#).
- [131] S. Kraml, T. Q. Loc, D. T. Nhung, and L. D. Ninh, “Constraining new physics from Higgs measurements with Lilith: update to LHC Run 2 results,” *SciPost Phys.* **7** (2019) 052, [arXiv:1908.03952 \[hep-ph\]](#).
- [132] G. Alguero, J. Heisig, C. Khosa, S. Kraml, S. Kulkarni, A. Lessa, H. Reyes-González, W. Waltenberger, and A. Wongel, “Constraining new physics with SModelS version 2,” [arXiv:2112.00769 \[hep-ph\]](#).
- [133] J. Alwall, R. Frederix, S. Frixione, V. Hirschi, F. Maltoni, O. Mattelaer, H. S. Shao, T. Stelzer, P. Torrielli, and M. Zaro, “The automated computation of tree-level and next-to-leading order differential cross sections, and their matching to parton shower simulations,” *JHEP* **07** (2014) 079, [arXiv:1405.0301 \[hep-ph\]](#).
- [134] **ATLAS** Collaboration, G. Aad *et al.*, “Search for new phenomena in events with an energetic jet and missing transverse momentum in pp collisions at $\sqrt{s} = 13$ TeV with the ATLAS detector,” *Phys. Rev. D* **103** (2021) 112006, [arXiv:2102.10874 \[hep-ex\]](#).
- [135] **DELPHI** Collaboration, J. Abdallah *et al.*, “Searches for supersymmetric particles in e^+e^- collisions up to 208-GeV and interpretation of the results within the MSSM,” *Eur. Phys. J. C* **31** (2003) 421–479, [arXiv:hep-ex/0311019](#).
- [136] J.-M. Zheng, Z.-H. Yu, J.-W. Shao, X.-J. Bi, Z. Li, and H.-H. Zhang, “Constraining the interaction strength between dark matter and visible matter: I. fermionic dark matter,” *Nucl. Phys. B* **854**

- (2012) 350–374, [arXiv:1012.2022 \[hep-ph\]](#).
- [137] **PICO** Collaboration, C. Amole *et al.*, “Dark Matter Search Results from the Complete Exposure of the PICO-60 C₃F₈ Bubble Chamber,” *Phys. Rev. D* **100** (2019) 022001, [arXiv:1902.04031 \[astro-ph.CO\]](#).
- [138] J. R. Ellis, M. K. Gaillard, and D. V. Nanopoulos, “A Phenomenological Profile of the Higgs Boson,” *Nucl. Phys. B* **106** (1976) 292.